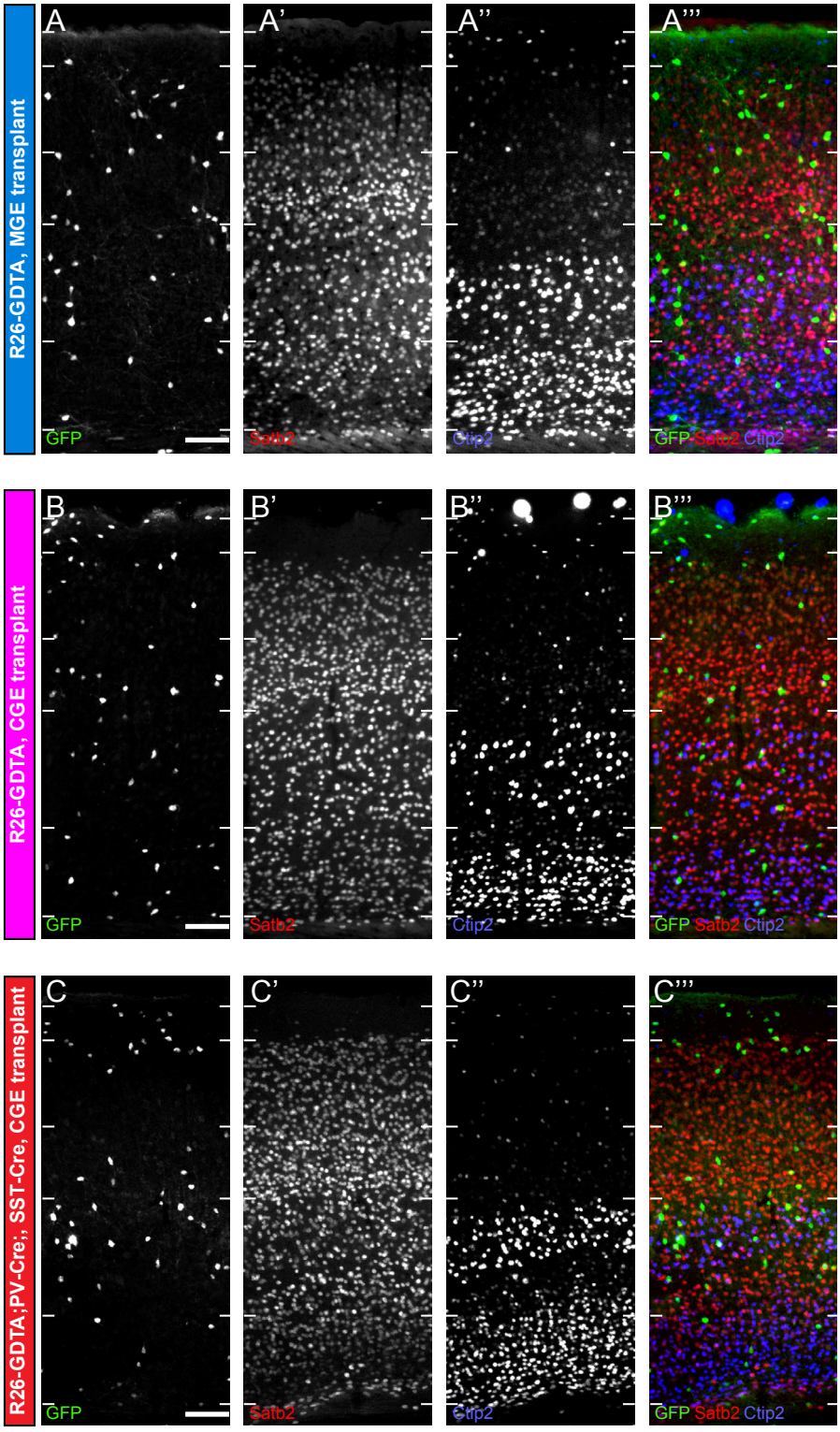

Figure S1, Related to Figure 1. The Transcription Factors Satb2 and Ctip2 Identify Cortical Laminae

Transplant derived neurons (A-C) from MGE (A), anatomically isolated CGE (B), or genetically isolated CGE (C) are found in all laminae as demonstrated by Satb2 (A'-C') and Ctip2 (A''-C'') staining.

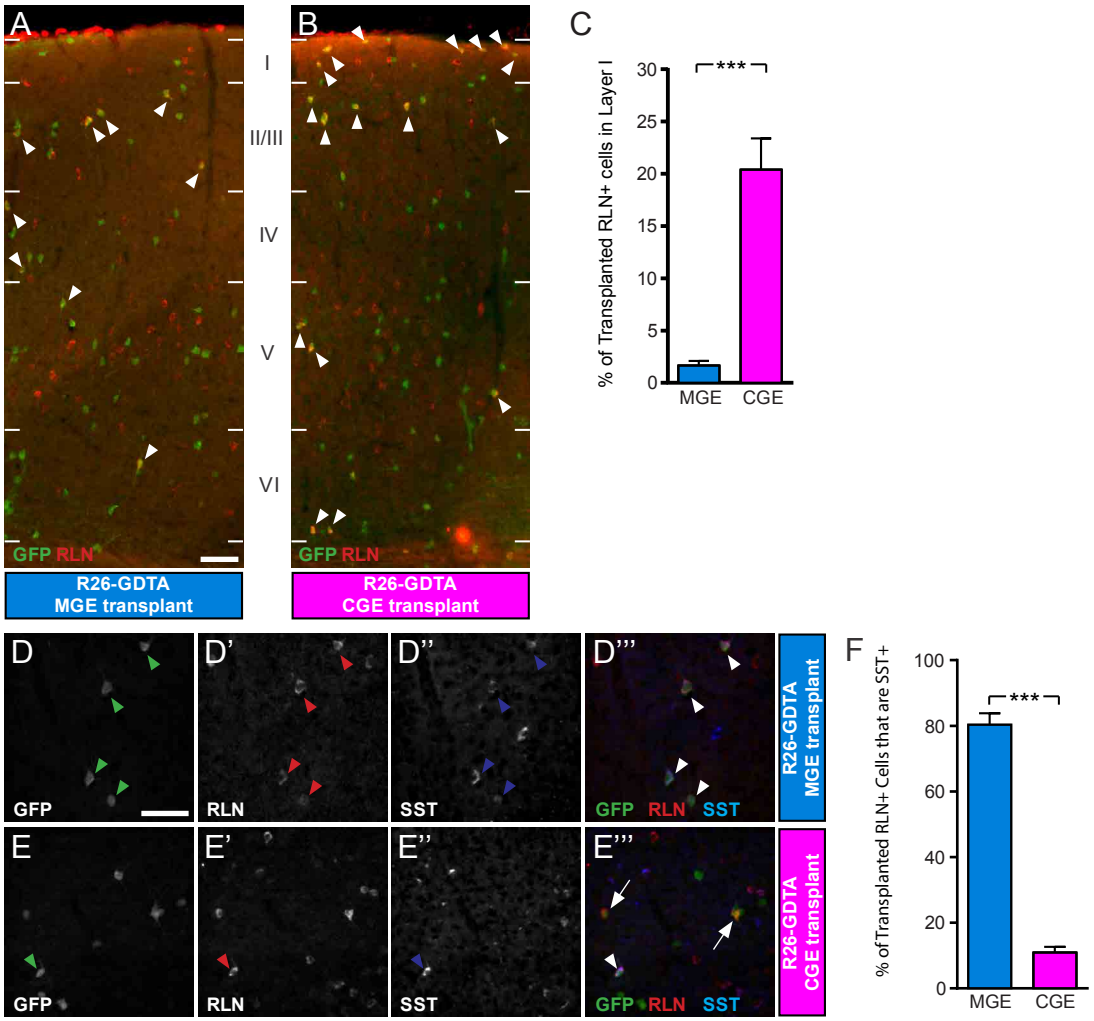

Figure S2, Related to Figure 2. MGE- and CGE-derived Reelin-Expressing Neurons Are Distinct

(A,B) Visual cortex coronal sections of R26-GDTA MGE (A) and CGE (B) cell transplant recipients stained for GFP and RLN. Arrowheads identify double-labelled cells. Scale bar: 100 μm.
(C) Percent of transplanted RLN cells that localize to Layer I in MGE and CGE recipients, respectively, at 35DAT. Error bars represent SEM (4 recipient mice of each type; t-test, *** $p<0.001$).
(D,E) Visual cortex coronal sections stained for GFP (D,D''',E,E'''), RLN (D',D''',E',E''') and SST (D'',D''',E'',E''') at 35DAT illustrating the presence of neurons co-expressing RLN and SST in both MGE and CGE cell transplant recipients at 35DAT.
(F) Percent of transplanted RLN cells that co-express SST in MGE and CGE recipients, respectively, at 35DAT. Error bars represent SEM (4 recipient mice of each type; t-test, *** $p<0.001$).

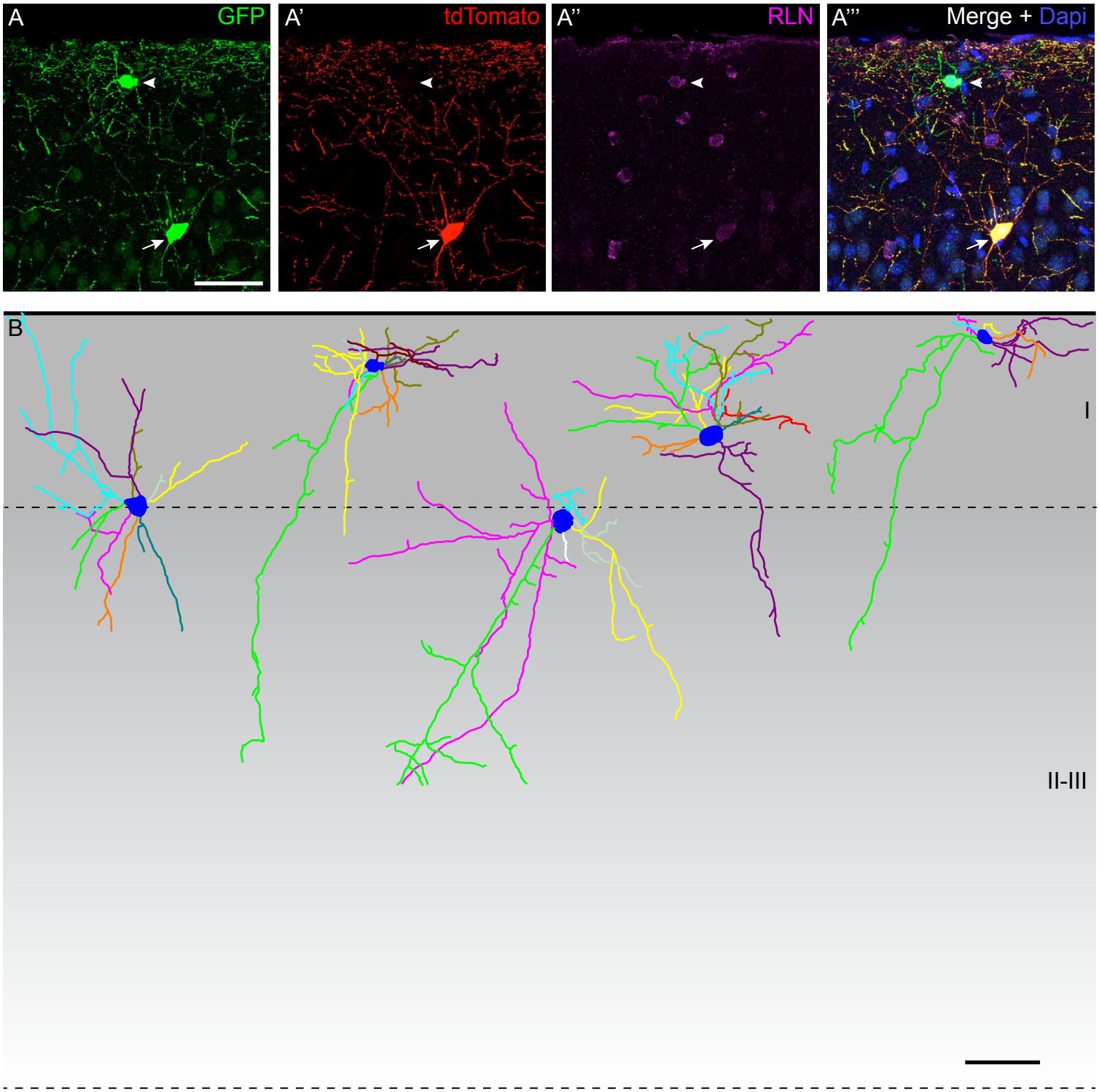

Figure S3, Related to Figure 2. Reelin Immunoreactive Neurons Demonstrate Neurogliaform Morphologies

(A) MGE and CGE cells from donor mice expressing GFP ubiquitously and tdTomato specifically in MGE lineage neurons (Nkx2.1-Cre; R26-Ai14; β-actin-GFP) were harvested at E13.5 and transplanted into the visual cortex of P5 hosts. 200 µm thick brain sections were stained for GFP (A), tdTomato (A'), and RLN (A''). The arrowhead identifies a RLN+ transplant-derived CGE lineage neuron. The arrow identifies a RLN+ transplant-derived MGE lineage neuron. Scale bar: 50 µm.
(B) Example morphological reconstructions of RLN+ transplant-derived CGE lineage neurons. Z-stack images were acquired on a confocal microscope using 200 µm thick brain sections. Tracing was performed using Neurolucida (MBF Bioscience) and relied on GFP staining. Neurite color distinguishes branches of each neuron. Scale bar: 50 µm.

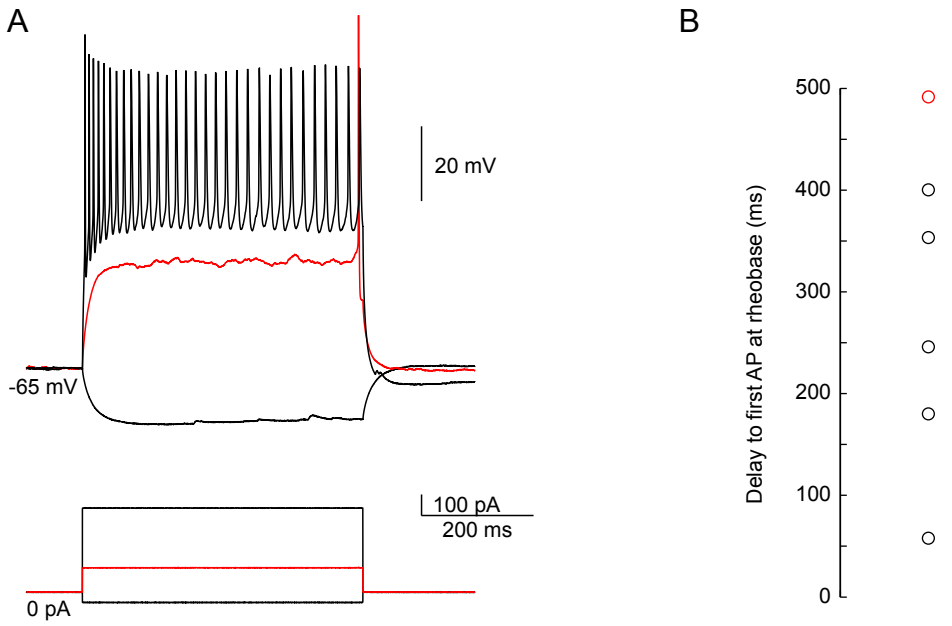

Figure S4, Related to Figure 3. Layer 1 Neurogliaform Neurons Derived From Genetically Identified CGE Transplants Demonstrate Typical Late-Spiking Phenotypes

We recorded from layer I neurons using Alexa680 in our intracellular solution to verify neurogliaform morphology after post-fixing. These neurons tended to be late spiking, and also demonstrated other passive and active electrophysiological parameters in line with those published previously (resting membrane potential -63±4 mV, input resistance 390±70 MΩ, membrane tau 24±5 ms, action potential threshold -39±3 mV, action potential width 1.1±0.1 ms, afterhyperpolarization amplitude -14±2 mV, delay to first spike at rheobase 288±64 ms for 500 ms step, maximum firing frequency 68±7 Hz, n=6 cells in two animals).

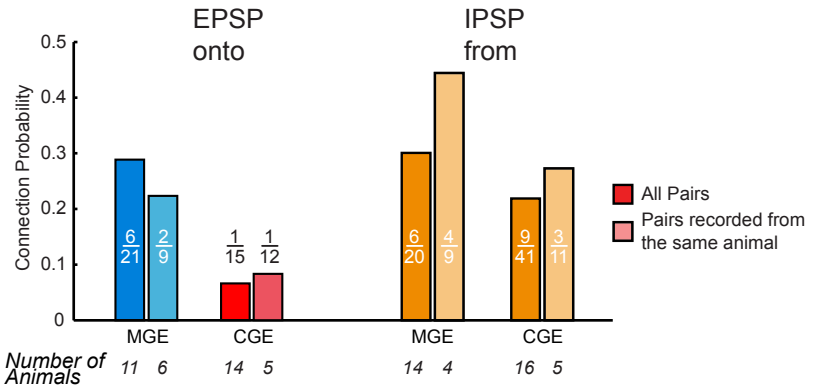

Figure S5, Related to Figures 4 and 5. MGE And CGE Connectivity Are Similar Between The Subset Of Recordings In Which MGE And CGE Neurons Were Recorded In The Same Animal, And The Total Population of Paired Recordings

To assess functional integration of CGE-derived interneurons into host cortex, we performed paired intracellular recordings of transplant-derived and host neurons at ~35 DAT. We used either dual MGE/CGE transplants (Nkx2.1;Ai14;β-actin-GFP, n=17 mice, to label all transplant derived neurons with GFP and only MGE derived neurons with tdTomato), or MGE-depleted CGE transplants (Nkx2.1-Cre;R26-GDTA, n=9 mice). The former mating allowed direct comparison between MGE and CGE transplant derived interneuron connectivity as they could be recorded in the same slice (48% of connections tested). The latter mating leads to the death of MGE derived interneurons thus generating transplants with only CGE lineage neurons. The connections from transplant derived neurons to pyramidal neurons for both types of transplants (number of connections found over number of connections tested) were not statistically different (connection probabilities by Fisher exact test; amplitude, latency, PPR by Mann Whitney; $p>0.05$), which indicates that CGE transplant connectivity is not modified by the presence of MGE-derived interneurons within the transplant. Thus data from these two transplants were pooled in the analyses for Figures 4 and 5.

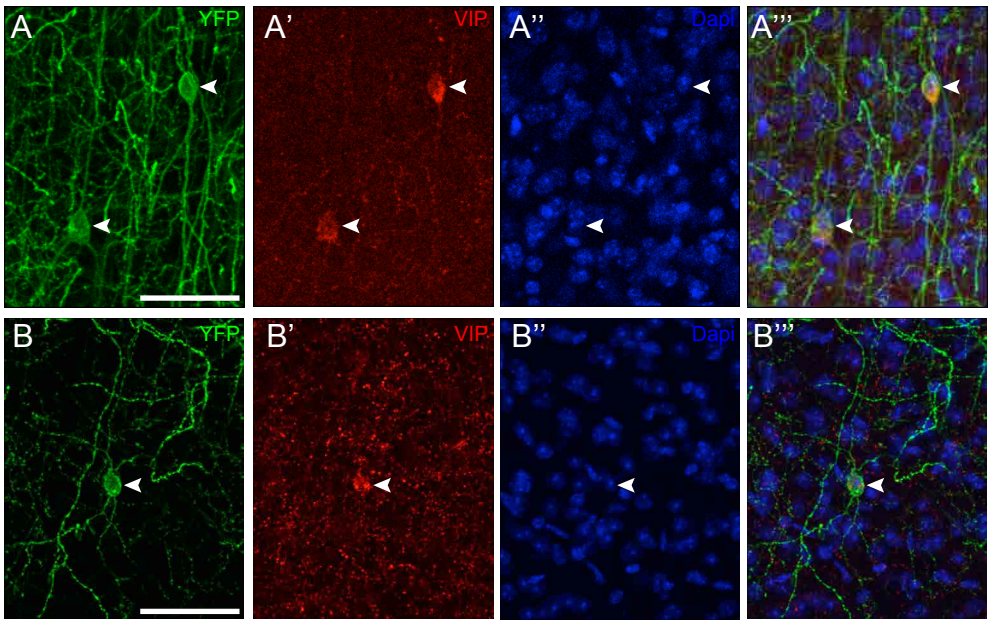

Figure S6, Related to Figure 6. VIP-Cre Driven Floxed Genes Colocalize with VIP in Transplant Derived Neurons During Adulthood

(A) Coronal brain section from an adult VIP-Cre;R26-Ai32 adult mouse stained for YFP and VIP and thus illustrating specific Cre-dependent YFP expression from the R26-Ai32 allele in VIP+ interneurons. Arrowheads identify VIP interneurons expressing YFP. Scale bar: 50µm. (B) CGE cells from donor mice expressing YFP specifically in VIP interneurons (VIP-Cre; R26-Ai32) were harvested at E13.5 and transplanted into the visual cortex of P5 hosts. Coronal 50µm-thick brain sections from recipient animals were stained for YFP and VIP at 75DAT. The arrowhead identifies a VIP+ CGE transplant-derived neuron expressing YFP. Scale bar: 50µm.

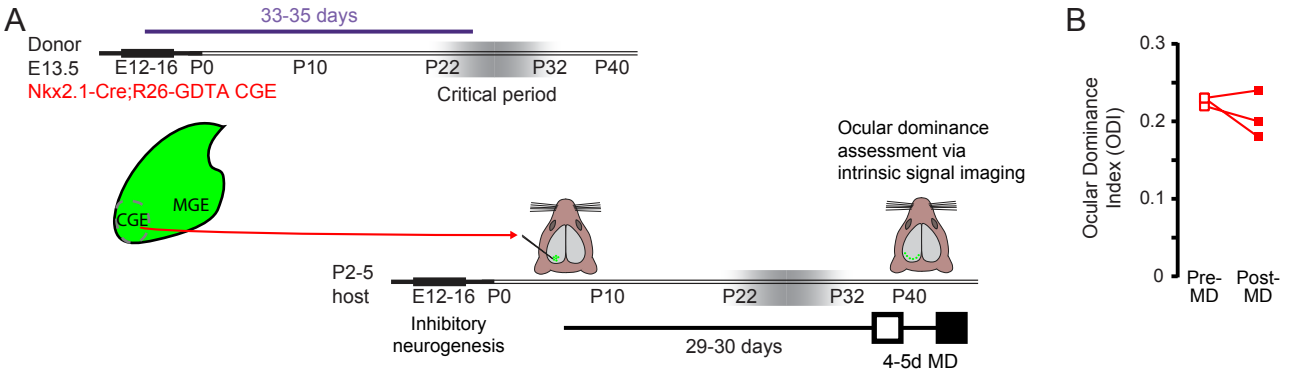

Figure S7, Related to Figure 7. Nkx2.1-Cre;R26-GDTA CGE Recipients Do Not Exhibit A Heterochronic Critical Period

(A) CGE cells from Nkx2.1-Cre;R26-GDTA donors were dissected at E13.5, dissociated, and transplanted into the visual cortex of P7 hosts. Animals were imaged before and after a 4-5 day period of monocular deprivation starting at 29-30DAT.
(B) Ocular dominance index before and after MD of the contralateral eye (n=3 mice) (Mann-Whitney test, p=0.60).

Supplemental Experimental Procedures

Animals. All protocols and procedures followed the guidelines of the Animal Care and Use Program at the University of California, San Francisco. All mice were housed in standard conditions on a 12H dark/light cycle in the Laboratory Animal Resource Center at the University of California, San Francisco. R26-Ai14, β-actin-GFP, Gad67-GFP, Nkx2.1-Cre, SST-Cre, PV-Cre, VIP-Cre, R26-GDTA, and wild-type C57BL/6J breeders were purchased from The Jackson Laboratory.

Cell Dissection and Transplantation: The ventricular and subventricular zones of the MGE and/or CGE were dissected from E13.5-E14.5 donor embryos and dissociated by repeated pipetting in Leibovitz's L-15 medium containing 100U/mL DNase I (Roche). Dissociated cells were concentrated via centrifugation (800 x g for 3 minutes). P5-8 recipients were anesthetized via hypothermia until pedal reflex disappeared and then placed on a stereotaxic platform for injection of concentrated cells (200-350 cells/nL, 300 nL per injection for 120-200k cells total injected) through a beveled Drummond glass micropipette (Drummond Scientific) positioned at 30° from vertical. Two injections were placed into the caudal left cortex at 7 mm posterior, 3.5 mm lateral and 6.5 mm posterior, 3.2 mm lateral, as measured from the inner corner of the eye (for anterior zero) and midpoint between the two eyes (for midline zero). Injections were made at 0.8-1.2 mm deep from the skin surface. After injection, recipients were placed on a heating pad until warm and active at which time they were returned to their mothers until weaning (P21).

Immunostaining: Animals were transcardially perfused first with ice-cold PBS and then with a solution of 4% PFA prepared in PBS. The brains were harvested, postfixed for 2-4 hours in a solution of 4% PFA (in PBS) and cryoprotected by immersion in a PBS solution containing 30% sucrose. 40μm coronal brain sections were cut using a sliding microtome (Leica & Physitemp Instruments). Free-floating sections were blocked for a minimum of 1 hour at room temperature in a blocking solution containing tris-buffered saline, 10% normal goat serum, and 1% Triton X-100. They were then incubated overnight at 4°C with one or more of the following primary antibodies and dilutions: chicken anti-GFP (AvesLab), 1:1000; mouse anti-PV (Sigma, Parv19), 1:1000; rabbit anti-SST (Swant), 1:300; goat anti-SST (Santa Cruz), 1:200; rabbit anti-calbindin (Millipore), 1:1000; rabbit anti-calretinin (Millipore), 1:1000; rabbit anti-NPY (Abcam), 1:1000; rabbit anti-reelin (Abcam), 1:1000; rabbit anti-VIP (Immunostar), 1:1000; mouse anti-Satb2 (Abcam), 1:500; rat anti-Ctip2 (Abcam), 1:500. After washing in TBS and 1% Triton X-100 three times for 15 minutes each, sections were incubated in blocking solution with appropriate Alexa secondary antibodies (Life Technologies) at 1:2000 for 1 hour at room temperature. They were then washed three times in TBS and 1% Triton X-100 for 15 minutes each prior to mounting on glass slides and coverslipping.

Cell Counting: Images of the binocular visual cortex as demarcated by DiI injections after functional imaging were captured using a Zeiss Axiovert-200 microscope (Zeiss), an AxioCam MRm camera (Zeiss), and Neurolucida (MBF Bioscience). Cell density was defined as the number of fluorescent cells within the binocular visual cortex divided by the total area as defined by DiI injections.

Monocular Deprivation: Monocular deprivation was produced by suturing the right eyelid shut for 4 days (checked daily to confirm eyelid closure).

Intrinsic Signal Imaging: Two to four days prior to imaging, mice were anesthetized with 2.5% isoflurane and the skull over left visual cortex was exposed then protected with nitrocellulose (MedTech Products). A stainless steel head plate was attached via dental acrylic and mice were given 5 mg/kg carprofen for postoperative analgesia prior to return to their home cage. For imaging, mice were anesthetized with 0.7% isoflurane and a single i.p. injection of 2-5 mg/kg chlorprothixene. The headplate was secured to a stereotaxic frame and agarose topped with a coverslip was applied to the skull to provide a flat imaging surface. Animals were maintained at 37.5°C (as measured by rectal thermometer) and eyes were protected with silicone oil. A Dalsa 1M30 CCD camera focused 550 μm deep to cortical surface vessels collected 610 nm light reflected by the visual cortex through the skull. At the conclusion of the final imaging session, the boundaries of the binocular cortex as determined by intrinsic signal imaging were marked with a thin tungsten wire coated with DiI (Invitrogen).

Analysis of Intrinsic Signal Data: Visual response amplitude was defined as the average signal amplitude for each pixel and ODI was computed as (C-I)/(C+I) where C is the response to contralateral visual stimulation and I is the

response to ipsilateral visual stimulation. Mean ODI is calculated as the average ODI of all pixels in the imaged field.

Animal Preparation for Calcium Imaging: AAV-2/5-CAG-flex-GCaMP6s (UPenn Vector Core) was injected stereotaxically at P30 as described previously (Fu et al., 2014) into the primary visual cortex (V1) of mice that had been transplanted at P2 with donor CGE cells from *VIP-Cre;R26-Ai14* embryos. In brief, a dental drill was used to generate a burr hole in the skull over the binocular zone of primary visual cortex in anesthetized mice. A 10-30 μm glass micropipette was lowered below the pial surface to the specified coordinates, and 0.5-1 μL of virus was injected using a Picospritzer (50 ms pulses over 5 min). The micropipette was left in place for three additional minutes to allow virus diffusion, after which the pipette was removed and the scalp closed with Vetbond (3M).

In Vivo, Two-Photon Calcium Imaging: Approximately 3 weeks after virus injection, a custom titanium head plate with a 5 mm-diameter window was affixed to the skull over V1 and a circular glass coverslip (3 mm diameter) was cemented over a craniotomy, under isoflurane anesthesia (3% induction, 1.5 – 2% maintenance) supplemented with subcutaneous analgesic injections. Imaging experiments were performed 3-7 days after window implantation. Animals were maintained at 37 °C by a feedback-controlled heating pad. GCaMP6 signal was collected using a custom modified Movable Objective Microscope (Sutter Instrument) equipped with a Chameleon ultrafast laser (920 nm) and controlled by ScanImage. Images were collected at 5 Hz, 512 x 256 pixels, from the depth between 150 and 300 μm below the cortical surface (approximately layer 2/3, one z plane per recording set). Regions of interest (ROIs) corresponding to visually identifiable cell bodies were selected based on the expression of *tdTomato*. The fluorescence time course of each cell was obtained in ImageJ by averaging all pixels within the ROI. Further analyses were performed using a custom written Matlab program (Fu et al., 2014). Briefly, $\Delta F/F_0$ was calculated as $(F-F_0)/F_0$, where F_0 is the baseline fluorescence signal averaged over a 2-s period immediately before the start of visual stimulation. Peak visual responses were measured for each trial as $\Delta F/F_0$, averaged over the last 2 s of the stimulus period. Neurons were considered visually responsive when fluorescence changes were significantly related to the stimulus (ANOVA across blank and 12 direction stimulus periods, $P < 0.01$) (Ohki et al., 2005), with an average $\Delta F/F_0$ at preferred orientations greater than 10%. The orientation selectivity index (OSI) was computed for responsive cells as:

$$\frac{\sqrt{\left(\sum R(\theta_i) * \sin\left(2\theta_i\right)\right)^2 + \left(\sum R(\theta_i) * \cos\left(2\theta_i\right)\right)^2}}{\sum R(\theta_i)}$$

where θ_i is the orientation of each stimulus and $R(\theta_i)$ is the response to that stimulus (Fu et al., 2014).

Visual Stimuli. Stimuli were displayed on an LCD monitor (Dell, 30x40 cm, 60Hz refresh rate, 32 cd/m^2 mean luminance) placed 25 cm from the mouse (-5° to +15° azimuth). For intrinsic signal evaluation of ocular dominance, a black-and-white contrast-modulated stochastic noise movie was presented to the binocular visual field. Each movie was presented five times to each eye alternately for 5 minutes per presentation. For evaluation of orientation selectivity, drifting sinusoidal grating stimuli were generated using the Psychophysics Toolbox extensions (Brainard, 1997; Pelli, 1997) in Matlab with each trial stimulus consisting of a 3 s grating (0.05 cycle per degree, 1 Hz temporal frequency) followed by a 4 s blank period of uniform 50% gray. Twelve drifting directions in 30° steps presented in random sequence were repeated 6 times per recording set.

Slice Preparation. Transplantation was performed at P2-8 and slices of host brains were prepared at 32-39 DAT (P35-43), the time of greatest transplant-induced plasticity seen with MGE transplants. Animals were overdosed with pentobarbital, decapitated, and the brain was removed into ice-cold dissection buffer containing (in mM): 234 sucrose, 2.5 KCl, 10 $MgSO_4$, 1.25 NaH_2PO_4, 24 $NaHCO_3$, 11 dextrose, 0.5 $CaCl_2$, bubbled with 95% O_2 / 5% CO_2 to a pH of 7.4. Coronal slices of the primary visual cortex (300 μm thick) were prepared with a vibratome and transferred to a holding chamber filled with artificial cerebrospinal fluid (ACSF) containing (in mM): 124 NaCl, 3 KCl, 2 $MgSO_4$, 1.23 NaH_2PO_4, 26 $NaHCO_3$, 10 dextrose, 2 $CaCl_2$ (bubbled with 95% O_2 / 5% CO_2) and incubated at 33°C for 30 min then stored at room temperature until slices were transferred to a flow chamber for recording.

Electrophysiology. Whole-cell recordings were made in current-clamp mode with a Multiclamp 700B or AxoClamp 2B amplifier (Molecular Devices) using an internal solution that contained (in mM): 140 K gluconate, 2 $MgCl_2$, 10 HEPES, 0.2 EGTA, 4 MgATP, 0.3 NaGTP, 10 phosphocreatine (290 mOsm, pH 7.3). Neurons were visualized

using IR-DIC video microscopy with fluorescent excitation of *GFP* and *tdTomato* provided by a mercury lamp. Data were filtered at 10 kHz and digitized at 5-10 kHz by a 16 bit analog-to-digital converter (National Instruments). Data acquisition and analysis were done with custom software written in Matlab. The estimated chloride equilibrium was -91 mV (not corrected for the liquid junction potential). Input resistance was monitored throughout recordings with small hyperpolarizing pulses and recordings were discarded if input resistance changed by >50% or if the membrane potential became unstable. Neuron input resistance and spiking properties were characterized using brief current pulses (-50 to 400 pA, 500 ms). For some neurons (12 percent of total connections tested), a loose-patch configuration was used. For a subset of transplanted neurons, extracellular stimulation (constant voltage, 2-5V for 200 μs) in superjacent layer 1 with a bipolar tungsten electrode was used to elicit a minimal postsynaptic response.

Analysis of Intrinsic Electrophysiological Properties: For analysis of synaptic potentials we used a threshold crossing method developed previously (Cohen and Miles, 2000) and described in detail elsewhere (Larimer and Strowbridge, 2008). Input resistance was calculated from steady-state responses to small hyperpolarizing (~10 mV) responses to current pulses. Action potential threshold was determined as the earliest point where the second derivative of the voltage with respect to time was >10% of the peak second derivative during the rising phase of the action potential. Action potential height was measured from threshold to peak. Action potential duration was measured at the voltage midpoint between action potential threshold and peak. ISI was measured using the time of action potential peaks, with accommodation assessed by the ratio of the last ISI to the first. Cells were included in the final analysis if they had action potential amplitudes greater than 40 mV and one cell with an apparent input resistance of 2 GΩ was also eliminated from the dataset. All analyses were implemented in Matlab. Cell electrophysiological phenotype was defined by comparing the ISIs over the duration of a 500 ms depolarizing pulse that elicited approximately half the maximum number of action potentials for that neuron to the categorizations defined by the Petilla Interneuron Nomenclature Group (Ascoli et al., 2008).

Statistical Analysis: For cell densities and lamination a t-test was used with Bonferroni correction. Transplant dispersion was assessed using a Kruskal-Wallace test. For proportion of synaptic connections, significance was determined with a two-sided Fisher exact test (as implemented by R). For all other two-way comparisons, a Mann Whitney was used, with Bonferroni correction for multiple comparisons. All other statistical tests were performed using Matlab. All data are presented as mean±SEM unless otherwise noted.

Supplemental References

Ascoli, G.A., Alonso-Nanclares, L., Anderson, S.A., Barrionuevo, G., Benavides-Piccione, R., Burkhalter, A., Buzsáki, G., Cauli, B., Defelipe, J., Fairén, A.*, et al.* (2008). Petilla terminology: nomenclature of features of GABAergic interneurons of the cerebral cortex. Nat. Rev. Neurosci. *9*, 557-568.

Brainard, D.H. (1997). The Psychophysics Toolbox. Spat. Vis. *10*, 433-436.

Cohen, I., and Miles, R. (2000). Contributions of intrinsic and synaptic activities to the generation of neuronal discharges in in vitro hippocampus. J. Physiol. *524* Pt 2, 485-502.

Fu, Y., Tucciarone, Jason M., Espinosa, J.S., Sheng, N., Darcy, Daniel P., Nicoll, Roger A., Huang, Z.J., and Stryker, Michael P. (2014). A Cortical Circuit for Gain Control by Behavioral State. Cell *156*, 1139-1152